Fruit ripening-associated leucylaminopeptidase with cysteinylglycine dipeptidase activity from durian suggests its involvement in glutathione recycling

Pawinee Panpetch
Chulalongkorn University
Supaart Sirikantaramas (supaart.s@chula.ac.th)
Chulalongkorn University Faculty of Science https://orcid.org/0000-0003-0330-0845

Research article

Keywords: durian, leucylaminopeptidase, LAP, sulphur compound, Cys-Gly, fruit ripening

Posted Date: May 3rd, 2020

DOI: https://doi.org/10.21203/rs.3.rs-25816/v1

Version of Record: A version of this preprint was published on February 1st, 2021. See the published version at https://doi.org/10.1186/s12870-021-02845-6.

Abstract

Background

Durian (*Durio zibethinus* M.) is a highly popular fruit in Thailand and several other Southeast Asian countries. It is abundant in essential nutrients and several sulphur-containing compounds such as glutathione (GSH) and γ-glutamylcysteine (γ-EC). Cysteinylglycine (Cys-Gly) generated by GSH catabolism is also found in durian fruit pulp. Cysteine (Cys) is a precursor of the sulphur-containing volatiles produced during durian fruit ripening and accounting for the strong odour and flavour of the ripe fruit. However, the genes encoding plant Cys-Gly dipeptidases have seldom been identified. Our aim was to analyse the Cys-Gly peptidase activity of leucylaminopeptidase (LAP) in durian fruit pulp.

Results

DzLAP1 and *DzLAP2* were identified, which the former was highly expressed in the fruit pulp. *DzLAP1* expression at various ripening stages and in response to ethephon/1-MCP treatments suggested that *DzLAP1* is active and important at the early stages of fruit ripening. Biochemical characterisation showed that DzLAP1 is a metalloenzyme activated by Mg^{2+} or Mn^{2+}, is approximately 63 kDa in size, and has an optimal alkaline pH of 9.5 which is typical of LAPs. Kinetic studies revealed that DzLAP1 had a Km of 1.62 mM for its preferred substrate Cys-Gly. DzLAP1-GFP was localised to the cytosol and targeted to the plastids.

Conclusions

DzLAP1 has Cys-Gly dipeptidase activity in the γ-glutamyl cycle. The present study discloses that the LAPs identified in durian fruit pulp are implicated in the high sulphur-containing compound levels observed at full ripening.

Background

Durian (*Durio zibethinus* M.) is a highly flavourful fruit grown in Thailand and other Southeast Asian countries. Production and export of fresh durian and its products are highly profitable. Several studies showed that durian is abundant in protein, carbohydrate, and fat [1] as well as bioactive phenolic and anti-proliferative compounds [2–4]. Durian fruit has a unique texture, flavour, and odour. Several sulphur-containing volatiles are responsible for the pungent odour of ripe durian fruit. Glutathione (GSH), gamma-glutamylcysteine (γ-EC), *S*-adenosylmethionine (SAM), cysteine (Cys), and cysteinylglycine (Cys-Gly) were detected in the ripe fruit pulp of two popular Thai durian cultivars Chanee and Monthong [5]. However, Chanee apparently has a stronger odour and faster postharvest ripening than Monthong. Moreover, ripe Chanee fruit has higher Cys and Cys-Gly levels than ripe Monthong fruit [5].

Cys-Gly is an important dipeptide intermediate in the so-called gamma-glutamyl cycle of sulphur metabolism. Cys-Gly participates in redox homeostasis and recycles amino acids in living cells. In

mammals, Cys-Gly is the product of GSH degradation via sequential reactions of γ-glutamyl transpeptidase (GGT), γ-glutamyl cyclotransferase (GGCT), and 5-oxoprolinase (OPase) [6]. Nevertheless, only the concerted actions of GGCT and OPase or a GGT-independent pathway were associated with Cys-Gly production in *Arabidopsis* [7]. Cys-Gly is then hydrolysed by dipeptidase to yield Cys and Gly. Cys-Gly is a thiol with pro-oxidant activity that could contribute to the intracellular redox environment. Excess Cys-Gly was toxic to yeast cells [8, 9]. Therefore, enzymatic regulation of the Cys-Gly level is probably vital to the cell. Moreover, release of the sulphur-containing amino acid Cys is important as it can be converted to methionine to produce sulphur volatiles in durian fruit ripening [10].

Leucylaminopeptidases (LAPs, EC. 3.4.11.1) are M17 family peptidases. They may process and turn over intracellular proteins but their precise functions in cellular metabolism remain to be determined. It has been reported that they preferentially hydrolyse Cys-Gly in *Bos taurus* (cow) [11], *Treponema denticola* [12], and *Arabidopsis* [13]. They were originally named as LAPs because early reports suggested that they rapidly react with *N*-terminal leucines in peptide chains [14]. Cytosolic Dug1p, a metallopeptidase M20 family member, has Cys-Gly peptidase activity. Its homologues are found in mammals and yeast but not plants [15]. LAPs are homomeric enzymes with six identical monomers consisting of two conserved zinc-binding sites per subunit [16]. They participate in amino acid turnover but their other biological functions in various species are somewhat complex and species-specific. *Escherichia coli* LAP (also known as XerB, PepA, or CarP) is an aminopeptidase-independent DNA-binding protein [17, 18]. It mediates site-specific plasmid and phage recombination [19, 20] and transcriptional *carAB* operon activation [18]. Multiple functions have been reported for mammalian LAPs. High LAP accumulation was detected in response to interferon-γ (IFN-γ) induction. Hence, LAP may participate in antigen presentation in human cells [21, 22]. Animal LAPs have been implicated in lens aging caused by oxidative damage [23]. Certain plant LAPs such as LAP-A are defence proteins and play important roles in floral development in tomato, potato, and other Solanaceae [24–27].

Plant LAPs are classified as acidic LAP-A and neutral LAP-N according to their pI. LAP-A and LAP-N have distinctly different biochemical properties and respond differently to various developmental and environmental cues. LAP-A is found only in the Solanaceae. It is induced by biotic and abiotic stress [28–30] and accumulates to high concentrations in the reproductive organs [31, 32]. In contrast, LAP-N is constitutively produced in all plants [30, 32]. *LAP-A*-silenced tomatoes were comparatively more susceptible to *Manduca sexta* (tomato hornworm) invasion than their wild type counterparts [33]. Both LAP-A and LAP-N are molecular chaperones that protect proteins from heat damage (Scranton et al. 2012). Here, we identified two LAP isoforms in durian fruit pulp. The only highly expressed isoform in the durian fruit pulp was the LAP-N DzLAP. We biochemically characterised DzLAP1 expressed as a His-tagged protein in *E. coli*. Our objective was to clarify its cooperative function in sulphur-volatile compound production by liberating Cys from preferential Cys-Gly cleavage. We demonstrated the dual localisation of DzLAP1 in the cytoplasm and chloroplast and examined its physiological roles in cytosolic GSH metabolism and plastidial peptide catabolism. To the best of our knowledge, the present study is the first to associate DzLAP1 with durian fruit ripening.

Results

Identification of LAPs, protein sequence alignment, and phylogenetic analysis

To search for the *LAP*s in durian, we used the protein sequences of a spirochete bacterium (TdLAP) and *Arabidopsis* (AtLAP1 and AtLAP3) as queries for tblastn against the open-source genome database of the Musang King durian cultivar. We identified *DzLAP1_MK* and *DzLAP2_MK*. Only one Chanee *DzLAP* isoform was present in our in-house RNA-seq data obtained from ripe pulp tissues (data not shown). The full-length Chanee DzLAP was multiply aligned with those of Musang King and tomato (*Solanum lycopersicum*; SlLAP1 and SlLAP2), potato (*Solanum tuberosum*; StLAP1 and StLAP2), and *Arabidopsis* (*Arabidopsis thaliana*; AtLAP1 to AtLAP3). We annotated the putative Chanee *DzLAP* as *DzLAP1* (accession no. MN879753) encoding DzLAP1 which was represented as DzLAP1_CN in multiple alignment and phylogenetic NJ. DzLAP1_CN clustered with Musang King DzLAP1_MK. DzLAP1 shared 99.3% and 89.7% identity with DzLAP1_MK and DzLAP2_MK, respectively. Eight highly conserved residues (K350, D355, K362, D375, D435, E437, R439, and L463 of DzLAP1) involved in substrate binding or catalytic function were observed (Fig. 1, arrowheads). LAPs are metallopeptidases. Five conserved residues (K350, D355, D375, D435, and E437) interacted with metal ions [34, 35]. The latter are crucial enzyme cofactors. The aforementioned conserved residues constitute a subset of the catalytic residues (Fig. 1, boxes). All protein sequences including DzLAP1 (but neither SlLAP1 nor StLAP1) harboured substitutions of all 28 LAP-A signature residues (data not shown). Fully conserved residues were present in the *C*-terminal region containing all of the essential active residues participating in catalysis (Fig. 1, asterisks). In contrast, the *N*-terminal region harboured highly variable amino acid sequences [32]. Except for AtLAP1, which lacked the signal peptide sequence, the *N*-terminal regions of SlLAPs and StLAPs were slightly shorter than the other sequences. Only ~ 64–77% identity was established when the SlLAP and StLAP sequences were compared with those of *Arabidopsis* and durian.

A phylogenetic analysis revealed that all plant LAPs were clustered together and separate from those of bacteria (Fig. 2). However, Cys-Gly peptidase activity was observed in certain plant and bacterial LAPs. Tomato (SlLAPs) and potato (StLAPs) LAPs (Solanaceae) were grouped apart from those of *Arabidopsis* and durian and demonstrated various metabolic functions such as defence responses and protein catabolism (Fig. 2). On the other hand, they had little activity towards Cys-Gly [28]. Comparison of several LAPs revealed that they resided in different cellular compartments and may have had different putative functions (Fig. 2).

Gene expression analysis by qRT-PCR

In silico analysis of *DzLAP_MK* expression varied substantially among tissue types. *DzLAP1_MK* had the highest expression level in durian pulp whereas *DzLAP2_MK* was expressed in other tissues (Supplementary Fig. S1). Therefore, we focused on *DzLAP1_MK* as it was nearly identical to Chanee *DzLAP1*. The qRT-PCR disclosed the relative *DzLAP1* expression patterns at the unripe, midripe, and ripe stages in Chanee and Monthong durian fruit pulp. *DzLAP1* was significantly upregulated from the unripe

to midripe stages but was downregulated by the ripe stage (Fig. 3a). *DzLAP1* expression in the Chanee cultivar (white bars) slightly resembled that for the Monthong cultivar (black bars) (Fig. 3a). To validate the association between *DzLAP1* and durian fruit ripening, we applied the phytohormones ethephon and 1-MCP. *DzLAP1* was significantly downregulated in durian fruit pulp treated with 1-MCP relative to those undergoing natural ripening (control) or accelerated ripening (ethephon) (Fig. 3b). The ethephon treatment had relatively little influence on *DzLAP1* expression.

rDzLAP1 production and biochemical characterisation in vitro

The purified soluble rDzLAP1 produced by *E. coli* appeared as a single-band protein on SDS gel. Its molecular weight was ~ 63 kDa which was confirmed by western blot (Fig. 4a). The concentration of purified DzLAP1 was ~ 1.16 mg mL^{-1} relative to the BSA standard.

The metalloenzyme activity of DzLAP1 was tested by incubating it with Cys-Gly substrate in the presence of Ca^{2+}, Zn^{2+}, Mg^{2+}, Ni^{2+}, and Mn^{2+}. The enzyme activity was measured by a modified acidic ninhydrin method wherein released cysteines are detected. The highest enzyme activity was determined for the reaction systems containing Mg^{2+} and Mn^{2+}. Conversely, Ca^{2+}, Zn^{2+}, and Ni^{2+} had minimal or negligible effect because the enzyme activity in their presence did not significantly differ from that measured for the metal ion-free control reaction system (Fig. 4b). Thus, Mg^{2+} was selected as the DzLAP1 cofactor in the enzyme kinetics assay. The optimal enzyme pH was established by incubating DzLAP1 with Cys-Gly at pH 4.0–11.0. DzLAP1 had maximum activity against Cys-Gly at pH 9.5 (Fig. 4c). Approximately 80% of the enzyme activity occurred within a pH range of 8.0–11.0. At pH < 7.0, the enzyme activity was < 50%. Under acidic conditions (pH 4.0–5.0), DzLAP1 was inactive.

To identify enzyme substrate specificity, we incubated 3.5 µg purified rDzLAP1 with various concentrations of substrates in the presence of 1 mM $MgCl_2$ + 25 mM K_3PO_4 buffer (pH 8.0) at 37 °C for a specific length of time. There was no enzyme activity when tripeptide GSH and γ-linked dipeptide (γ-Glu-Cys) were used as substrates (Table 1). As DzLAP1 had positive activity against various α-linked dipeptide substrates, it was proposed that this enzyme is a Cys-Gly dipeptidase because its catalytic efficiency was highest in the presence of Cys-Gly. Its k_{cat}/Km for Cys-Gly was ~ 118 × and ~ 6 × higher than those for Met-Gly and Leu-Gly, respectively (Table 1). Nonetheless, a previous report indicated that LAP had preferential activity for *N*-terminal Leu peptides and high affinity for Leu-Gly (Km = 0.35 mM) [28].

Subcellular DzLAP1 localisation in N. benthamiana

An in silico analysis predicted that DzLAP1 was a chloroplast-localised protein. The pGWB5-*DzLAP1* and the silencing suppressor *p19* were co-expressed in *A. tumefaciens* GV3101 infiltrated in four-week-old *N. benthamiana* leaves. The in planta assay showed that GFP-tagged DzLAP1 was not membrane-bound but rather a soluble protein probably localised to the cytosol (Fig. 5). Fluorescence signals were detected

in the chloroplasts (Fig. 5, insets). These results suggest that durian DzLAP1 may be localised to either compartment.

Discussion

Durian fruit pulp accumulates large quantities of GSH [5]. GSH is vital for plant cell homoeostasis [36] and serves as a storage form of Cys via incorporation with Glu and Gly in the γ-glutamyl cycle [37]. Cys is recycled from Cys-Gly hydrolysis. The latter dipeptide is a by-product of GSH breakdown via LAP. We hypothesise that this mechanism generates large amounts of precursors of the fruit-ripening phytohormone ethylene as well as considerable quantities of sulphur-volatile compounds via methionine synthesis. Taken together, both pathways lead to durian fruit ripening and its associated malodour. Cys-Gly was also detected in durian fruit pulp [5]. For these reasons, the γ-glutamyl cycle must be activated in durian fruit ripening. Our aims, then, were to identify and characterise the DzLAPs possibly involved in the aforementioned biochemical processes. To date, there has been limited information on the participation of Cys-Gly dipeptidase in the γ-glutamyl cycle [13, 15].

LAPs are highly conserved metallopeptidases in animals, plants, and microorganisms [38]. Several *LAP*s have been identified in *Arabidopsis* [13] and durian (this work). *Arabidopsis* has three *LAP*s encoding AtLAP1–AtLAP3. In the durian cv. Musang King genome [10], *DzLAP1_MK* and *DzLAP2_MK* were found. Based on transcriptome data, we focused on *DzLAP1_MK* as it was highly expressed in the durian fruit pulp (Supplementary Fig. S1) where numerous sulphur compounds such as GSH and γ-EC accumulate [5]. *DzLAP1_MK* showed 99.3% identity with *DzLAP1* in the Chanee durian cultivar. The latter was the only isoform detected in our in-house RNA-seq data. The primary protein sequence analysis (Fig. 2) confirmed that DzLAP1 is a LAP-N because it contains all the conserved substrate binding/catalytic- and metal ion-binding residues responsible for the mechanism of this enzyme.

Postharvest *DzLAP1* expression analyses showed upregulation at the midripe stage. Thus, DzLAP1 may hydrolyse Cys-Gly to Cys and Gly which results in the strong malodour associated with durian pulp during ripening. The relative *DzLAP1* expression levels were similar for both Chanee and Monthong at each ripening stage (Fig. 3a). However, the Cys-Gly content in Chanee was significantly higher than that in Monthong ($p < 0.01$) [5]. Therefore, *DzLAP1* is neither cultivar-dependent nor the key gene accounting for the relative differences in odour intensity between Chanee and Monthong. As the competitive ethylene inhibitor 1-MCP significantly repressed *DzLAP1* during postharvest ripening ($p < 0.05$) (Fig. 3b), *DzLAP1* must play an important role in durian fruit ripening. These observations imply for the first time that *LAP1* is associated with the early stages of ripening. In contrast, the *LAP-N*s in other plants are constitutively expressed in all organs [32, 39]. To clarify *LAP* expression during fruit ripening, we compared their expression levels in tomato fruit. The *LAP-A* expression levels in tomato fruit at the breaker or ethylene-producing stages were slightly lower than those in mature green fruit (Supplementary Fig. S2a). Tomato *LAP-N* is constitutively expressed at all fruit developmental stages (Supplementary Fig. S2b). Thus, *LAP*s are not implicated in tomato fruit development or ripening.

An in vitro biochemical assay of rDzLAP1 disclosed that LAPs have pH optima in the weakly to moderately alkaline range (pH 8.0–11.0) and metal ion dependency [27, 40, 41]. Thus, DzLAP1 is a metalloenzyme. We also predicted the in vivo substrate(s) for DzLAP1. This enzyme showed apparently high catalytic efficiency (k_{cat}/Km) for Cys-Gly (Km = 1.6 mM). Therefore, DzLAP1 is a Cys-Gly dipeptidase. The aforementioned Km closely resembled those for other Cys-Gly peptidases such as AtLAP1 [13], yeast Dug1p [15], and bacterial TdLAP [12]. All of these were ≤ 1.3 mM. Thus, the affinity of LAP for Cys-Gly is relevant to the range of millimolar physiological GSH concentrations in living cells [42, 43]. Durian is GSH-rich compared to many other fruits and vegetables [5, 44]. For this reason, the cellular GSH level in durian should be higher than the general physiological concentration. This finding shows that Cys-Gly dipeptidases have highly conserved activity among various species. As with degradable α-linked dipeptides, DzLAP1 could not hydrolyse γ-Glu-Cys and GSH (γ-Glu-Cys-Gly) (Table 1). Consequently, this enzyme might have specificity for the α-peptide bonds in many cellular proteins. Nevertheless, previous studies did not investigate the affinities of LAPs for γ-linked dipeptide substrates.

Subcellular protein localisation could help clarify the correlation between the native functions and the physiological substrates of the enzyme. DzLAP1 is a dual-targeting protein localised to the chloroplasts and the cytosol (Fig. 5) even though it harbours a plastidial transit peptide sequence. *DzLAP1* transcripts might contain an alternative translation initiation codon for ribosomes that skip the first start codon [32] and/or form secondary RNA structures in the sequences surrounding the start codon [45]. Delta-2-isopentenyl pyrophosphate:tRNA isopentenyl transferase (MOD5) is encoded by a single gene, contains two translational initiation sites, and is located in the mitochondria, cytosol, and nuclei [46]. Plastidial DzLAP1 may perform important functions such as general protein recycling. The chloroplast is intimately involved in cellular metabolism. Thus, it might perceive and respond to various stressors [47]. Although a function of plastidial DzLAP1 was not clarified in this study, we anticipate its function as a molecular chaperone preventing certain negative effects such as misfolded protein accumulation. The latter function has been reported for AtLAPs [48]. In addition, the partial localisation of DzLAP1 observed in the chloroplasts strengthens its chaperone or protease activity in the specific suborganellar compartment. Similar observations have been reported for CRP-like protein (Clp) and filamentous temperature-sensitive protein (FtsH) that are the major conserved ATP-dependent proteases with chaperone and degradative functions compartmentalising in stroma and on thylakoid membranes, respectively [49]. Further functional experiments are needed to confirm its role in the plastids during ripening.

Cys-Gly has pro-oxidant activity. For this reason, its concentration must be regulated. Cys-Gly promotes the formation of reactive oxygen species such as hydrogen peroxide and superoxide anion in the presence of certain metal ions [50]. Thence, oxidation of several normally highly reduced thiol compounds including GSH is induced [51]. The cytosolic localisation and enzyme kinetic parameters of DzLAP1 suggest that it participates in Cys-Gly hydrolysis in the cytoplasmic γ-glutamyl cycle. In this way, DzLAP1 controls the cytosolic Cys-Gly levels. Moreover, Cys-Gly may be a substrate for cytosolic DzLAP1 in vivo and the enzyme effectively regulates its concentration. *DzLAP1* expression and localisation in the cytosol where ethylene and sulphur volatiles accumulate might indicate the involvement of this enzyme

in durian fruit ripening. The slightly alkaline pH optimum for DzLAP1 activity is consistent with the relatively basic cytoplasm [52] and chloroplast stroma [53, 54].

DzLAP1 shares certain important features of the LAP-N in *Arabidopsis* and Solanaceae including similar catalytic/substrate and metal ion-binding residues. However, the *DzLAP1* expression pattern differed from those of the other genes. Durian has evolved to accumulate high levels of sulphur compounds that impart a very strong and unique odour to the fruit. Nevertheless, the levels of these thiols must be tightly controlled. Therefore, expression of the genes encoding sulphur-metabolising enzymes must be regulated in durian fruit ripening. The *DzLAP1* promoter region may have been evolutionarily modified such that the optimal DzLAP1 content is produced to limit the amount of Cys-Gly and catalyse Cys recycling in order to the generation of sulphur volatiles and ethylene during fruit ripening. A similar finding was observed in the durian-specific gene expansion of methionine γ-lyase [10], a major enzyme responsible for sulphur volatile production in plants and microbes [55, 56]. A fruit ripening-associated isoform of this enzyme has been identified [10]. Taken together, we present a schematic diagram summarising the putative functions of DzLAP1 in the cytoplasm and chloroplasts of durian fruit pulp (Fig. 6).

Conclusions

Based on the durian cv. Musang King genomic data, we identified and characterised the LAP-N subfamily gene encoding leucylaminopeptidase (LAP) which is highly expressed in durian fruit pulp and was designated *DzLAP1*. We also established that *DzLAP1* is active in the early stages of durian fruit ripening. However, it is not cultivar-dependent and does not account for the fact that ripe Chanee durian fruit has a stronger odour than ripe Monthong durian fruit. Moreover, the kinetic values and subcellular localisation of *DzLAP1* indicate that it has Cys-Gly dipeptidase activity in vivo. Its presence in the cytosolic compartment suggests that it participates in the γ-glutamyl cycle and is in close proximity to the intracellular sites of ethylene and sulphur volatile production. The plastidial isoform of DzLAP1 might play vital roles in regular protein turnover and/or protein protection. Taken together, our findings initiate the process of elucidating plant sulphur metabolism mechanisms especially in tissues known to accumulate high volatile sulphur compound levels.

Methods

Plant materials and growth conditions

Mature durian (*Durio zibethinus* M.) cv. Chanee fruits were harvested from a commercial orchard in Trat Province, Thailand in early April 2017 at 95 d after anthesis. The samples were maintained at room temperature (30 °C) before being peeled on days 1, 2, and 4 which corresponded to the unripe, midripe, and ripe postharvest stages, respectively. Monthong was a representative sample for gene expression analysis and its three different ripening stages were also evaluated. However, its postharvest ripening stage timings (days) slightly differed from those of Chanee. The Monthong fruits were harvested at day

105 after anthesis and their unripe, midripe, and ripe samples were peeled and analysed one, three, and five days after storage at room temperature, respectively [57].

To investigate the association between *DzLAP1* with durian fruit ripening, unripe Monthong samples were treated either with the synthetic plant growth regulators ethephon or 1-methylcyclopropene (1-MCP). These phytohormones have opposite modes of actions. The treated samples were then compared with control samples naturally ripened according to the method of Khaksar et al. (2019). Ethephon is converted to ethylene which, in turn, enhances ripening. In contrast, 1-MCP inhibits or delays ripening. Three biological replicates were used and each of them was defined as a single durian fruit harvested from a separate tree.

Nicotiana benthamiana plants were raised for agroinfiltration. Seeds were sown on peat moss and grown under controlled conditions at 25 °C under a 16 h/8 h light/dark photoperiod (4,500 lx, artificial light). Two-week-old plants were individually transplanted to pots and left to grow under the aforementioned conditions for another 2 wks.

Phylogenetic analysis and putative LAP identification in durian

Protein sequences of well-characterised LAPs harbouring Cys-Gly dipeptidase activity in *Treponema denticola* (accession no. WP_010698434.1) [12] and *Arabidopsis thaliana* (AtLAP1 and AtLAP3; accession nos. P30184.1 and Q8RX72.1, respectively) [13] served as query sequences to conduct a BLAST search against the publicly accessible *D. zibethinus* cv. Musang King NCBI database. The MaGenDB database [58] was used to confirm all *DzLAP* isoforms.

To investigate the phylogenetic relationships among the LAPs from various sources, the amino acid sequences of the putative DzLAPs and other LAPs deposited in NCBI were subjected to ClustalW multiple alignment and a neighbour joining (NJ) tree was created with MEGA7 software [59] using 1,000 bootstrap replicates.

Determination of tissue-specific DzLAP expression

After searching the *DzLAP*s against the genomic data for durian cultivar Musang King, two candidate genes (accession nos. XM_022894525.1 (LOC111299369) and XM_022874012.1 (LOC111284913)) were found and annotated as *DzLAP1-like*. Here, these two isoforms were distinguished by renaming them as *DzLAP1_MK* and *DzLAP2_MK*, respectively. Attention was directed to the durian fruit pulp wherein several sulphur compounds accumulated. The expression levels of the aforementioned gene were analysed in various fruit tissues *in silico*. To compare the relative expression levels of the *DzLAP* in the different tissues, normalised total read counts (RCs) derived from Illumina reads were obtained from the public Sequence Read Archive (SRA) resource and processed according to the method of Khaksar et al. (2019). RNA-seq data were obtained for SRX3188225 (root), SRX3188222 (stem), SRX3188226 (leaf), and

SRX3188223 (aril/pulp) [10]. A heatmap was constructed according to the RCs with MetaboAnalyst v. 4.0 [60].

Gene expression analysis by quantitative real time polymerase chain reaction (qRT-PCR)

Total RNA was isolated from the Chanee and Monthong durian cultivar pulps with PureLink® Plant RNA Reagent (Thermo Fisher Scientific, Waltham, MA, USA), following the manufacturer's instructions. DNase-treated RNA sample quantity and integrity were assessed. Approximately 1 μg total RNA was reverse-transcribed to cDNA using a RevertAid First Strand cDNA Synthesis Kit (Thermo Fisher Scientific, Waltham, MA, USA) and the gene-specific primers listed in Supplementary Table S1. The qRT-PCR was performed to elucidate the *DzLAP1* expression patterns of unripe, midripe, and ripe durian fruit. The reactions were conducted in 10 μL total volume in a 96-well PCR plate. The cDNA and primers were combined with Luna® Universal qPCR Master Mix (New England Biolabs, Ipswich, MA, USA). The PCR was run with a CFX Connect™ Real-Time PCR Detection System and CFX Manager™ Software (Bio-Rad Laboratories, Hercules, CA, USA). Single amplicon production was verified by melting curve analysis. The relative gene expression levels were calculated by the $2^{-\Delta Ct}$ method [61] according to the cycle threshold (Ct) value of the gene compared with the reference gene, elongation factor 1 alpha (EF-1α). Three independent biological replicates were used in the qRT-PCR. Using the aforementioned procedures, gene expression analyses were also conducted on the ethephon- and 1-MCP-treated samples along with the naturally un/ripened samples (controls).

DzLAP1 **cloning and expression in** Escherichia coli

The putative *DzLAP1* was amplified with Phusion Hot Start II DNA polymerase (Thermo Fisher Scientific, Waltham, MA, USA) using midripe Chanee durian cultivar cDNA as a template. The PCR temperature profile was as follows: initial denaturation at 98 °C for 30 s; 30 cycles of 98 °C for 10 s; 57 °C for 10 s; 72 °C for 1 min; and a final extension at 72 °C for 5 min. Gene-specific forward and reverse primers were designed according to the *DzLAP1_MK* sequence (Supplementary Table S1) excluding the signal sequences predicted by the ChloroP1.1 and TargetP servers. The putative *DzLAP1* PCR product was excised with restriction enzymes (FastDigest™; Thermo Fisher Scientific, Waltham, MA, USA) and cloned into a pET21b vector (Merck KGaA, Darmstadt, Germany) to produce pET21b-*DzLAP1* in-frame with 18 nucleotides encoding 6 × His residues at the C-terminus. This recombinant plasmid was transformed into *E. coli* TOP10 (K2500-20; Invitrogen, Carlsbad, CA, USA). The bacterial colonies were raised on LB agar with 1 mg mL^{-1} ampicillin and subsequently analysed by colony PCR. The nucleotide sequences of the positive clones were verified (1st BASE DNA sequencing).

Recombinant DzLAP1 (rDzLAP1) production and purification

The pET21b-*DzLAP1* was transformed into the T7 host *E. coli* SoluBL21 (DE3). Cells harbouring the recombinant plasmid were incubated overnight in LB broth containing 1 mg mL^{-1} ampicillin. This starter

culture was then inoculated into fresh LB broth containing 1 mg mL^{-1} ampicillin and incubated at 37 °C with shaking at 250 rpm until OD_{600} = 0.4–0.5. The rDzLAP1 was generated by induction with 1 mM isopropyl β-D-1-thiogalactopyranoside (IPTG) at 30 °C and shaking for 17 h. The cells were harvested by centrifugation at 5,000 × g at 37 °C for 10 min, suspended in buffer A (25 mM K_3PO_4 buffer + 0.3 M NaCl; pH 7.2), and lysed by ultrasonication. Soluble intracellular proteins were collected by centrifugation at 7,500 × g and 4 °C for 30 min, analysed by western blot (6 × His Epitope Tag antibody; Thermo Fisher Scientific, Waltham, MA, USA), and stored at 4 °C until purification.

The crude extract was loaded onto a HisTrap™ column pre-equilibrated with buffer A. The column was washed with excess buffer A and the rDzLAP1 was eluted with buffer B (25 mM K_3PO_4 buffer + 0.3 M NaCl + 150 mM imidazole; pH 7.2). The samples were analysed by sodium dodecyl sulphate-polyacrylamide gel electrophoresis (SDS-PAGE) and western blot. The pooled purified rDzLAP1 fraction was dialysed against 25 mM K_3PO_4 buffer (pH 7.2). The protein concentration was determined by Bradford assay, with minor modifications [62]. The reference protein standard was bovine serum albumin (BSA).

Enzymatic rDzLAP1 assay

The metal ion dependency of rDzLAP1 was evaluated because this enzyme is a metallopeptidase. The rDzLAP1 was incubated at 37 °C for 15 min with 7.5 mM Cys-Gly in 25 mM K_3PO_4 buffer (pH 7.2) in the presence of 0 mM or 1 mM Ca^{2+}, Zn^{2+}, Mg^{2+}, Ni^{2+}, or Mn^{2+}. The total reaction volume was 50 µL. The enzyme activity was measured by a modified acidic ninhydrin method [63]. Briefly, the 50-µL enzyme reaction systems were terminated with 50 µL glacial acetic acid followed by 50 µL acidic ninhydrin solution (250 mg ninhydrin in 6 mL glacial acetic acid + 4 mL HCl), boiled for 9 min, and cooled with tap water. The pink endpoint colour was the product of the reaction between released Cys and ninhydrin under acidic conditions. Colour intensity was measured at A_{560}. The optimum enzyme pH was determined as follows. The 50-µL reactions were performed by incubating rDzLAP1 with 7.5 mM Cys-Gly and 1 mM Mg^{2+} at various pH (acetate buffer, pH 4–6; phosphate buffer, pH 6–8; Tris-HCl buffer, pH 8–9.5; glycine-NaOH buffer, pH 9.5–11) at 37 °C for 15 min. The maximum enzyme activity was defined as 100% relative activity.

To assess enzyme kinetics, 3.5 µg purified rDzLAP1 was incubated with 0–10 mM Cys-Gly, γ-Glu-Cys, GSH, Met-Gly, or Leu-Gly in the presence of 1 mM $MgCl_2$ in 25 mM K_3PO_4 buffer (pH 8.0) at 37 °C for a specific length of time. The reactions were terminated with 0.13 N HCl. For γ-Glu-Cys and GSH, the reactions were evaluated according to the aforementioned modified acidic ninhydrin assay. For Cys-Gly, Met-Gly, and Leu-Gly, the reactions were analysed by monitoring the decrease in low-UV absorbance (A_{230}) of the peptides after hydrolysis, with minor modifications [64]. The kinetic parameters were measured with OriginPro® 2017 software (OriginLab Corp., Northampton, MA, USA).

Subcellular localisation

Full-length *DzLAP1* was amplified with Phusion Hot Start II High-Fidelity DNA polymerase (Thermo Fisher Scientific, Waltham, MA, USA), using Chanee cDNA as a template. The gene-specific primers (excluding the stop codon) listed in Supplementary Table S1 were used for the PCR. The PCR product was cloned into a pCR™8/GW/TOPO® TA cloning vector (Invitrogen, Carlsbad, CA, USA) and generated pTOPO-*DzLAP1* which was then sequenced. The *DzLAP1* was transferred to the pGWB5 destination vector and fused at the *C*-terminal with green fluorescent protein (GFP) [65] via Gateway® LR Clonase® II (Invitrogen, Carlsbad, CA, USA). The pGWB5-*DzLAP1* product was transformed by electroporation into *Agrobacterium tumefaciens* GV3101.

Agrobacterium tumefaciens bearing the *DzLAP1-GFP* construct and *A. tumefaciens* with the silencing suppressor *p19* gene [66] were co-infiltrated into four-week-old plants as previously described. Briefly, cells from each culture were washed and suspended in MM buffer (10 mM MES buffer + 10 mM $MgCl_2$; pH 5.6). Cell suspensions harbouring *DzLAP1* and *p19* were adjusted at OD_{600} to optical densities of 0.8 and 0.6, respectively, and combined in a 1:1 ratio. Acetosyringone was added to the mixture to a final concentration of 200 μM and the suspension was maintained in darkness at room temperature for 2 h before infiltration. At day 3 after infiltration, autofluorescence was visualised under a FluoView® FV10i-DOC confocal laser scanning microscope (Olympus Corp., Tokyo, Japan). GFP, chloroplast autofluorescence, and phase-contrast detection excitation/emission were recorded at 473/510 nm, 559/600 nm, and 559/600 nm, respectively.

Statistical analyses

All data were analysed with SPSS Statistics® v. 22.0 software (IBM Corp., Armonk, NY, USA). One-way ANOVA was used to identify significant differences among treatment means for the average enzyme activity levels in the absence and presence of metal ions. The gene expression levels in the samples at various ripening stages and in those treated with different ripening regulators were analysed by Tukey's HSD multiple-comparisons test ($p < 0.05$).

Abbreviations

GSH
Glutathione
γ-EC
γ-glutamylcysteine
Cys-Gly
Cysteinylglycine
Cys
Cysteine
LAP
Lueucylaminopeptidase
DzLAP

Durio zibethinus M. leucylaminopeptidase gene

Declarations

Ethics approval and consent to participate

Not applicable.

Consent for Publication

Not applicable.

Availability of data and material

The datasets used and/or analysed during the current study are available from the corresponding author on reasonable request.

Competing interests

The authors declare that they have no competing interests.

Acknowledgements

The authors thank Kittiya Tantisuwanichkul and Pinnapat Pinsorn for providing the durian cDNA samples. The authors also thank Dr. Gholamreza Khaksar and Lalida Sangpong for their assistance with the RNA-seq data analysis. The authors thank Tsuyoshi Nakagawa of Shimane University, Shimane, Japan for providing the Gateway® expression vector pGWB5 and Sophien Kamoun of Sainsbury Laboratory, Norwich, Norfolk, UK for providing *A. tumefaciens* GV3101 harbouring pJL3:*p19*.

Funding

This study was supported by the Thailand Research Fund (No. RSA6080021) and Chulalongkorn University (No. GRU 6203023003-1) (to S.S.) and the Second Century Fund (C2F) Postdoctoral Fellowship, Chulalongkorn University (to P.P). Each of the funding bodies granted the funds based on research proposals and had no influence on the experimental design, data collection, analysis and interpretation, or on writing the manuscript.

Authors' contributions

S.S. conceived the study. P.P. and S.S. designed the experiments. P.P. conducted the experiments. P.P. and S.S. analysed the data and prepared the manuscript. All authors have read and approved the manuscript.

References

1. Charoenkiatkul S, Thiyajai P, Judprasong K. Nutrients and bioactive compounds in popular and indigenous durian (*Durio zibethinus* murr.). Food Chem. 2016;193:181–6.
2. Arancibia-Avila P, Toledo F, Park Y-S, Jung S-T, Kang S-G, Heo BG, Lee S-H, Sajewicz M, Kowalska T, Gorinstein S. Antioxidant properties of durian fruit as influenced by ripening. LWT-food Sci Technol. 2008;41:2118–25.
3. Maninang JS, Lizada MCC, Gemma H. Inhibition of aldehyde dehydrogenase enzyme by Durian (*Durio zibethinus* Murray) fruit extract. Food Chem. 2009;117:352–5.
4. Haruenkit R, Poovarodom S, Vearasilp S, Namiesnik J, Sliwka-Kaszynska M, Park Y-S, Heo B-G, Cho J-Y, Jang HG, Gorinstein S. Comparison of bioactive compounds, antioxidant and antiproliferative activities of Mon Thong durian during ripening. Food Chem. 2010;118:540–7.
5. Pinsorn P, Oikawa A, Watanabe M, Sasaki R, Ngamchuachit P, Hoefgen R, Saito K, Sirikantaramas S. Metabolic variation in the pulps of two durian cultivars: Unraveling the metabolites that contribute to the flavor. Food Chem. 2018;268:118–25.
6. Martin MN, Saladores PH, Lambert E, Hudson AO, Leustek T. Localization of members of the γ-glutamyl transpeptidase family identifies sites of glutathione and glutathione S-conjugate hydrolysis. Plant Physiol. 2007;144:1715–32.
7. Ohkama-Ohtsu N, Oikawa A, Zhao P, Xiang C, Saito K, Oliver DJ. A γ-glutamyl transpeptidase-independent pathway of glutathione catabolism to glutamate via 5-oxoproline in *Arabidopsis*. Plant Physiol. 2008;148:1603–13.
8. Kumar C, Igbaria A, D'autreaux B, Planson AG, Junot C, Godat E, Bachhawat AK, Delaunay-Moisan A, Toledano MB. Glutathione revisited: a vital function in iron metabolism and ancillary role in thiol-redox control. EMBO J. 2011;30:2044–56.
9. Srikanth CV, Vats P, Bourbouloux A, Delrot S, Bachhawat AK. Multiple *cis*-regulatory elements and the yeast sulphur regulatory network are required for the regulation of the yeast glutathione transporter, Hgt1p. Curr Genet. 2005;47:345–58.
10. Teh BT, Lim K, Yong CH, Ng CCY, Rao SR, Rajasegaran V, Lim WK, Ong CK, Chan K, Cheng VKY. The draft genome of tropical fruit durian (*Durio zibethinus*). Nat Genet. 2017;49:1633.
11. Cappiello M, Lazzarotti A, Buono F, Scaloni A, D'ambrosio C, Amodeo P, Méndez BL, Pelosi P, Del Corso A, Mura U. New role for leucyl aminopeptidase in glutathione turnover. Biochem J. 2004;378:35–44.
12. Chu L, Lai Y, Xu X, Eddy S, Yang S, Song L, Kolodrubetz D. A 52-kDa leucyl aminopeptidase from *Treponema denticola* is a cysteinylglycinase that mediates the second step of glutathione metabolism. J Biol Chem. 2008;283:19351–8.
13. Kumar S, Kaur A, Chattopadhyay B, Bachhawat AK. Defining the cytosolic pathway of glutathione degradation in *Arabidopsis thaliana*: role of the ChaC/GCG family of γ-glutamyl cyclotransferases as glutathione-degrading enzymes and AtLAP1 as the Cys-Gly peptidase. Biochem J. 2015;468:73–85.
14. Spackman DH, Smith EL, Brown DM. Leucine aminopeptidase IV. Isolation and properties of the enzyme from swine kidney. J Biol Chem. 1955;212:255–69.

15. Kaur H, Kumar C, Junot C, Toledano MB, Bachhawat AK. Dug1p is a Cys-Gly peptidase of the γ-glutamyl cycle of *Saccharomyces cerevisiae* and represents a novel family of Cys-Gly peptidases. J Biol Chem. 2009;284:14493–502.
16. Carpenter FH, Vahl JM. Leucine aminopeptidase (bovine lens) mechanism of activation by Mg^{2+} and Mn^{2+} of the zinc metalloenzyme, amino acid composition, and sulfhydryl content. J Biol Chem. 1973;248:294–304.
17. McCulloch R, Burke ME, Sherratt DJ. Peptidase activity of *Escherichia coli* aminopeptidase A is not required for its role in Xer site-specific recombination. Mol Microbio. 1994;12:241–51.
18. Charlier D, Kholti A, Huysveld N, Gigot D, Maes D, Thia-Toong T-L, Glansdorff N. Mutational analysis of *Escherichia coli* PepA, a multifunctional DNA-binding aminopeptidase. J Mol Biol. 2000;302:409–24.
19. Stirling C, Colloms S, Collins J, Szatmari G, Sherratt D: *xerB*, an *Escherichia coli* gene required for plasmid ColE1 site-specific recombination, is identical to pepA, encoding aminopeptidase A, a protein with substantial similarity to bovine lens leucine aminopeptidase. EMBO J. 1989;8:1623–1627.
20. Colloms SD: Leucyl aminopeptidase PepA. In: Handbook of proteolytic enzymes. Elsevier; 2004: 905–910.
21. Harris C, Hunte B, Krauss M, Taylor A, Epstein L. Induction of leucine aminopeptidase by interferon-gamma. Identification by protein microsequencing after purification by preparative two-dimensional gel electrophoresis. J Biol Chem. 1992;267:6865–9.
22. Towne CF, York IA, Neijssen J, Karow ML, Murphy AJ, Valenzuela DM, Yancopoulos GD, Neefjes JJ, Rock KL. Leucine aminopeptidase is not essential for trimming peptides in the cytosol or generating epitopes for MHC class I antigen presentation. J Immunol. 2005;175:6605–14.
23. Sharma KK, Kester K. Peptide hydrolysis in lens: role of leucine aminopeptidase, aminopeptidase III, prolyloligopeptidase and acylpeptidehydrolase. Curr Eye Res. 1996;15:363–9.
24. Hildmann T, Ebneth M, Peña-Cortés H, Sánchez-Serrano JJ, Willmitzer L, Prat S. General roles of abscisic and jasmonic acids in gene activation as a result of mechanical wounding. Plant Cell. 1992;4:1157–70.
25. Herbers K, Prat S, Willmitzer L. Functional analysis of a leucine aminopeptidase from *Solatium tuberosum* L. Planta. 1994;194:230–40.
26. Milligan SB, Gasser CS. Nature and regulation of pistil-expressed genes in tomato. Plant Mol Biol. 1995;28:691–711.
27. Chao WS, Gu Y-Q, Pautot V, Bray EA, Walling LL. Leucine aminopeptidase RNAs, proteins, and activities increase in response to water deficit, salinity, and the wound signals systemin, methyl jasmonate, and abscisic acid. Plant Physiol. 1999;120:979–92.
28. Gu YQ, Walling LL. Specificity of the wound-induced leucine aminopeptidase (LAP-A) of tomato: Activity on dipeptide and tripeptide substrates. Eur J Biochem. 2000;267:1178–87.

29. Gu Y-Q, Chao WS, Walling LL. Localization and post-translational processing of the wound-induced leucine aminopeptidase proteins of tomato. J Biol Chem. 1996;271:25880–7.
30. Chao WS, Pautot V, Holzer FM, Walling LL. Leucine aminopeptidases: the ubiquity of LAP-N and the specificity of LAP-A. Planta. 2000;210:563–73.
31. Pautot V, Holzer FM, Chaufaux J, Walling LL. The induction of tomato leucine aminopeptidase genes (*LapA*) after *Pseudomonas syringae* pv. tomato infection is primarily a wound response triggered by coronatine. Mol Plant Microbe In. 2001;14:214–24.
32. Tu C-J, Park S-Y, Walling LL. Isolation and characterization of the neutral leucine aminopeptidase (LapN) of tomato. Plant Physiol. 2003;132:243–55.
33. Hartl M, Merker H, Schmidt DD, Baldwin IT. Optimized virus-induced gene silencing in *Solanum nigrum* reveals the defensive function of leucine aminopeptidase against herbivores and the shortcomings of empty vector controls. New Phytol. 2008;179:356–65.
34. Kim H, Lipscomb WN. Differentiation and identification of the two catalytic metal binding sites in bovine lens leucine aminopeptidase by X-ray crystallography. Proc Nat Acad Sci. 1993;90:5006–10.
35. Dorus S, Wilkin EC, Karr TL. Expansion and functional diversification of a leucyl aminopeptidase family that encodes the major protein constituents of drosophila sperm. BMC Genom. 2011;12:177.
36. Foyer CH, Noctor G. Redox homeostasis and antioxidant signaling: a metabolic interface between stress perception and physiological responses. Plant Cell. 2005;17:1866–75.
37. May MJ, Vernoux T, Leaver C, Montagu MV, Inze D. Glutathione homeostasis in plants: implications for environmental sensing and plant development. J Exp Bot. 1998;49:649–67.
38. Rawlings ND, Barrett AJ: Introduction: metallopeptidases and their clans. In: Handbook of proteolytic enzymes. Elsevier; 2004: 231–267.
39. Bartling D, Nosek J. Molecular and immunological characterization of leucine aminopeptidase in *Arabidopsis thaliana*: a new antibody suggests a semi-constitutive regulation of a phylogenetically old enzyme. Plant Sci. 1994;99:199–209.
40. Mathew Z, Knox TM, Miller CG. *Salmonella enterica* serovar Typhimurium peptidase B is a leucyl aminopeptidase with specificity for acidic amino acids. J Bacteriol. 2000;182:3383–93.
41. Walling LL: Leucyl aminopeptidase (plant). In: Handbook of Proteolytic enzymes. Elsevier; 2004: 901–905.
42. Fahey R, Brown W, Adams W, Worsham M. Occurrence of glutathione in bacteria. J Bacteriol. 1978;133:1126–9.
43. Koffler BE, Bloem E, Zellnig G, Zechmann B. High resolution imaging of subcellular glutathione concentrations by quantitative immunoelectron microscopy in different leaf areas of *Arabidopsis*. Micron. 2013;45:119–28.
44. Wierzbicka GT, Hagen TM, Tones DP. Glutathione in food. J Food Compos Anal. 1989;2:327–37.
45. Yogev O, Pines O. Dual targeting of mitochondrial proteins: mechanism, regulation and function. BBA-Biomembranes. 2011;1808:1012–20.

46. Slusher LB, Gillman EC, Martin NC, Hopper AK: mRNA leader length and initiation codon context determine alternative AUG selection for the yeast gene *MOD5*. Proc Nat Acad Sci. 1991;88:9789–9793.
47. Van Aken O, De Clercq I, Ivanova A, Law SR, Van Breusegem F, Millar AH, Whelan J. Mitochondrial and chloroplast stress responses are modulated in distinct touch and chemical inhibition phases. Plant Physiol. 2016;171:2150–65.
48. Scranton MA, Yee A, Park S-Y, Walling LL. Plant leucine aminopeptidases moonlight as molecular chaperones to alleviate stress-induced damage. J Biol Chem. 2012;287:18408–17.
49. Nishimura K, Kato Y, Sakamoto W. Chloroplast proteases: updates on proteolysis within and across suborganellar compartments. Plant Physiol. 2016;171:2280–93.
50. Del Corso A, Vilardo PG, Cappiello M, Cecconi I, Dal Monte M, Barsacchi D, Mura U. Physiological thiols as promoters of glutathione oxidation and modifying agents in protein S-thiolation. Arch Biochem Biophys. 2002;397:392–8.
51. Glutathione. The *Arabidopsis* Book/American Society of Plant Biologists
9
Noctor G, Queval G, Mhamdi A, Chaouch S, Foyer CH. Glutathione. The *Arabidopsis* Book/American Society of Plant Biologists 2011, 9.
52. Martinière A, Bassil E, Jublanc E, Alcon C, Reguera M, Sentenac H, Blumwald E, Paris N. In vivo intracellular pH measurements in tobacco and *Arabidopsis* reveal an unexpected pH gradient in the endomembrane system. Plant Cell. 2013;25:4028–43.
53. Höhner R, Aboukila A, Kunz H-H, Venema K. Proton gradients and proton-dependent transport processes in the chloroplast. Front Plant Sci. 2016;7:218.
54. Su P-H, Lai Y-H. A reliable and non-destructive method for monitoring the stromal pH in isolated chloroplasts using a fluorescent pH probe. Front Plant Sci. 2017;8:2079.
55. Rébeillé F, Jabrin S, Bligny R, Loizeau K, Gambonnet B, Van Wilder V, Douce R, Ravanel S. Methionine catabolism in *Arabidopsis* cells is initiated by a γ-cleavage process and leads to S-methylcysteine and isoleucine syntheses. Proc Nat Acad Sci. 2006;103:15687–92.
56. Gonda I, Lev S, Bar E, Sikron N, Portnoy V, Davidovich-Rikanati R, Burger J, Schaffer AA, Tadmor Ya, Giovannonni JJ. Catabolism of L–methionine in the formation of sulfur and other volatiles in melon (*Cucumis melo* L.) fruit. Plant J. 2013;74:458–72.
57. Khaksar G, Sangchay W, Pinsorn P, Sangpong L, Sirikantaramas S. Genome-wide analysis of the *Dof* gene family in durian reveals fruit ripening-associated and cultivar-dependent Dof transcription factors. Sci Rep. 2019;9:1–13.
58. Wang D, Fan W, Guo X, Wu K, Zhou S, Chen Z, Li D, Wang K, Zhu Y, Zhou Y. MaGenDB: a functional genomics hub for Malvaceae plants. Nucleic Acids Res. 2020;48:D1076–84.
59. Kumar S, Stecher G, Tamura K. MEGA7: molecular evolutionary genetics analysis version 7.0 for bigger datasets. Mol Biol Evol. 2016;33:1870–4.

60. Chong J, Soufan O, Li C, Caraus I, Li S, Bourque G, Wishart DS, Xia J. MetaboAnalyst 4.0: towards more transparent and integrative metabolomics analysis. Nucleic Acids Res. 2018;46:W486–94.
61. Schmittgen TD, Livak KJ. Analyzing real-time PCR data by the comparative Ct method. Nat Protoc. 2008;3:1101.
62. Bradford MM. A rapid and sensitive method for the quantitation of microgram quantities of protein utilizing the principle of protein-dye binding. Anal Biochem. 1976;72:248–54.
63. Gaitonde M. A spectrophotometric method for the direct determination of cysteine in the presence of other naturally occurring amino acids. Biochem J. 1967;104:627.
64. Tombs M, Souter F, Maclagan N. The spectrophotometric determination of protein at 210 mμ. Biochem J. 1959;73:167.
65. Nakagawa T, Kurose T, Hino T, Tanaka K, Kawamukai M, Niwa Y, Toyooka K, Matsuoka K, Jinbo T, Kimura T. Development of series of gateway binary vectors, pGWBs, for realizing efficient construction of fusion genes for plant transformation. J Biosci Bioeng. 2007;104:34–41.
66. Lindbo JA. High-efficiency protein expression in plants from agroinfection-compatible Tobacco mosaic virus expression vectors. BMC Biotechnol. 2007;7:52.
67. Consortium TG. The tomato genome sequence provides insights into fleshy fruit evolution. Nature. 2012;485:635.

Table

Table 1: Kinetic parameters of DzLAP1 on different substrates

Substrate	k_{cat} (min^{-1})	Km (mM)	k_{cat}/Km (min^{-1} mM^{-1})
GSH	N.D.	N.D.	N.D.
γ-Glu-Cys	N.D.	N.D.	N.D
Cys-Gly	74.8 ± 8.1	1.6 ± 0.3	46.2
Met-Gly	2.1 ± 0.4	5.2 ± 1.3	0.4
Leu-Gly	2.9 ± 0.4	0.4 ± 0.1	8.2
Supplementary Table S1 Primers used in the present study. Restriction sites are underlined			

Supplementary Figure Legends

Supplementary Fig. S1 Tissue-specific expression profiles of the two *DzLAP*s in Musang King durian fruit pulp. *DzLAP1_MK* and *DzLAP2_MK* expression levels in fruit pulp, stem, leaf, and root were analysed by RNA-seq. Red: higher gene expression level; blue: lower gene expression level. Data were sum-normalised, log-transformed, and autoscaled

Supplementary Fig. S2 Relative *LAP-A* (a) and *LAP-N* (b) expression in tomato fruit at various developmental stages. *LAP-A* (Solyc12g010020) (a) and *LAP-N* (Solyc12g010040) (b) expression levels in tomato (*Solanum lycopersicum*) were obtained from Illumina-based and RPKM-normalised data [67] and represented in Tomato eFP Browser v. 2.0. The mature green, breaker, and breaker + 10 d tomato fruit ripening stages were compared

Figures

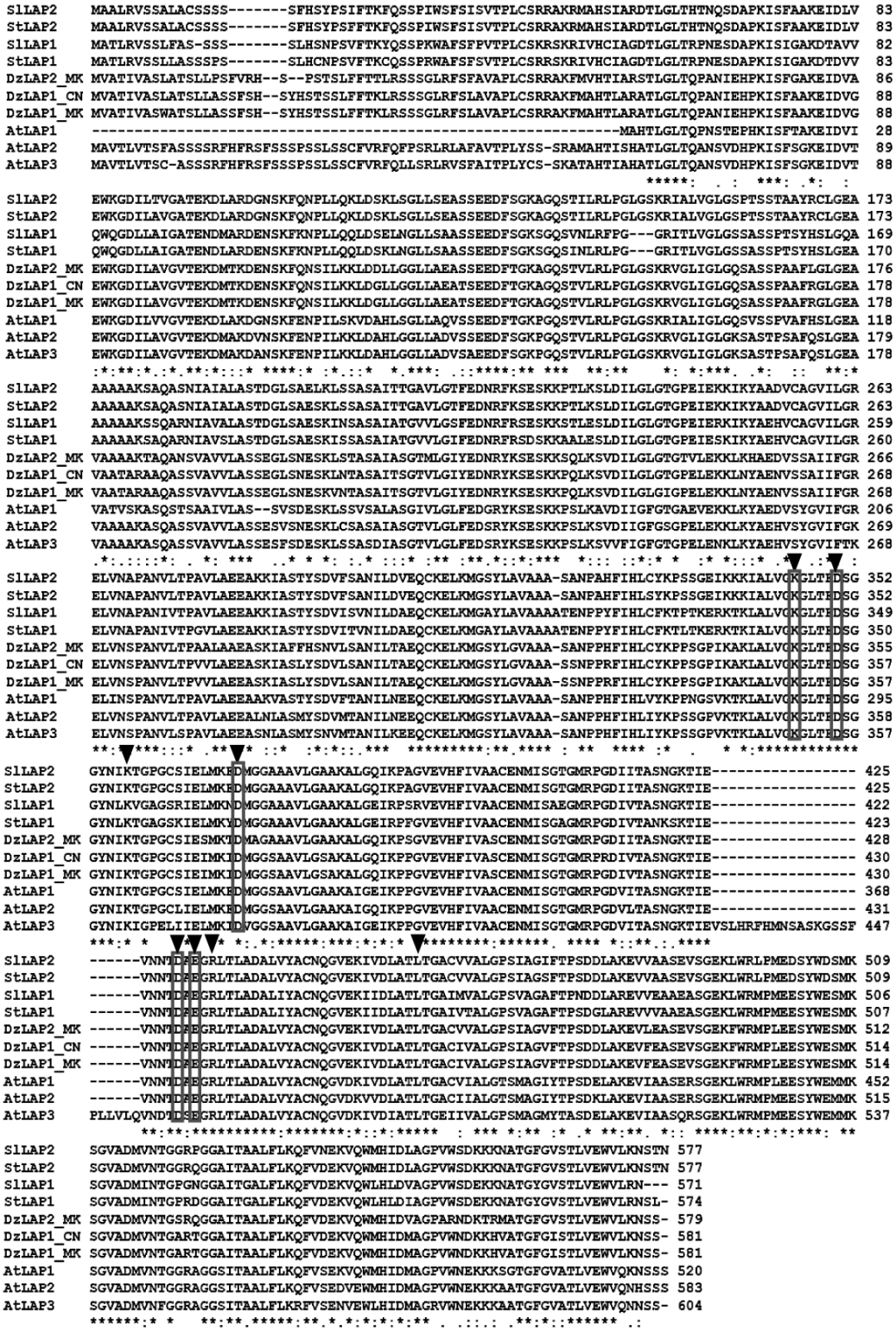

Figure 1

Amino acid sequence alignment of various plant LAPs. Deduced amino acid sequence of Chanee DzLAP1 (DzLAP1_CN) aligned with Musang King DzLAP1_MK and DzLAP2_MK (Durio zibethinus), AtLAP1 – AtLAP3 from Arabidopsis (Arabidopsis thaliana); StLAP1 and StLAP2 from potato (Solanum tuberosum); and SlLAP1 and SlLAP2 from tomato (Solanum lycopersicum). Eight substrate binding/catalytic residues marked by arrowheads. Five of eight residues are conserved metal ion-

coordinating residues (boxes). Asterisks, colons, and dots indicate strictly, highly, and moderately conserved amino acid residues, respectively

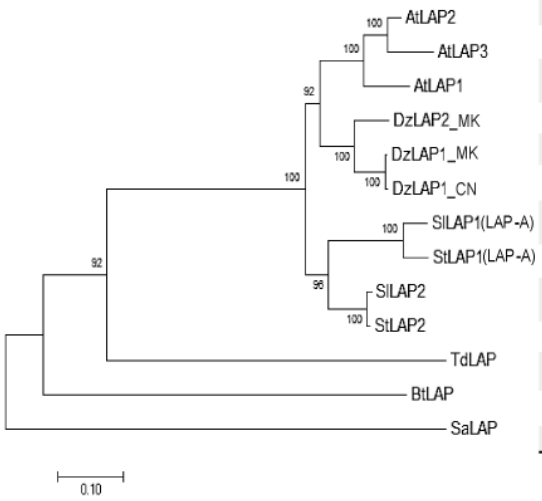

In silico prediction server SUBA3	ChloroP 1.1	TargetP 1.1	Experimental evidence	Substrate specificity/ Possible function	Reference
Chloro	-	-	Chloroplast proteome analysis	Molecular chaperone	Kumar et al. 2015; Scranton et al. 2012
Chloro	-	-	N.A.	Cys-Gly dipeptidase	Kumar et al. 2015
Cyto	-	-	Cytosolic proteome analysis	Cys-Gly dipeptidase; Molecular chaperone	Kumar et al. 2015; Scranton et al. 2012
-	Chloro	Chloro	-	N.A.	This work
-	Chloro	Chloro	-	N.A.	This work
-	Chloro	Chloro	Chloro/Cyto	Cys-Gly dipeptidase	This work
-	-	-	Chloro/Cyto	Defence response; wound signaling; Molecular chaperone	Gu et al. 1996; Scranton et al. 2012
-	-	-	Chloro/Mito	Senescence response	Herbers et al. 1994
-	-	-	Chloro/Cyto	Molecular chaperone	Narvaez-Vasquez et al. 2007; Scranton et al. 2012
-	-	-	Chloro/Mito	Protein turnover	Herbers et al. 1994
-	-	-	Cyto	Cys-Gly dipeptidase	Chu et al. 2008
-	-	-	Cyto	Cys-Gly dipeptidase	Cappiello et al. 2004
-	-	-	Cyto	Bacterial virulence	Carroll et al. 2013

Figure 2

Phylogenetic analysis and comparison of various LAPs. Neighbour-joining (NJ) tree constructed using MEGA 7 software with 1,000 bootstrap replicates. Arabidopsis thaliana: AtLAP1 (NP_179997), AtLAP2 (NP_194821), and AtLAP3 (NP_001328632); Solanum lycopersicum: SlLAP1 (NP_001233862.2) and SlLAP2 (NP_001233884.2); Solanum tuberosum: StLAP1 (XP_006350102.1) and StLAP2 (XP_015165363.1); Durio zibethinus: Musang King DzLAP1_MK (NW_019167860.1) and DzLAP2_MK (NW_019168159) and Chanee DzLAP1_CN (MN879753); Treponema denticola: TdLAP (WP_010698434.1); Bos Taurus: BtLAP (NP_776523.2); Staphylococcus aureus: SaLAP (ORO33369.1). Table on right represents locations of LAPs analysed either by in silico prediction or by empirical evidence and based on their presumptive roles

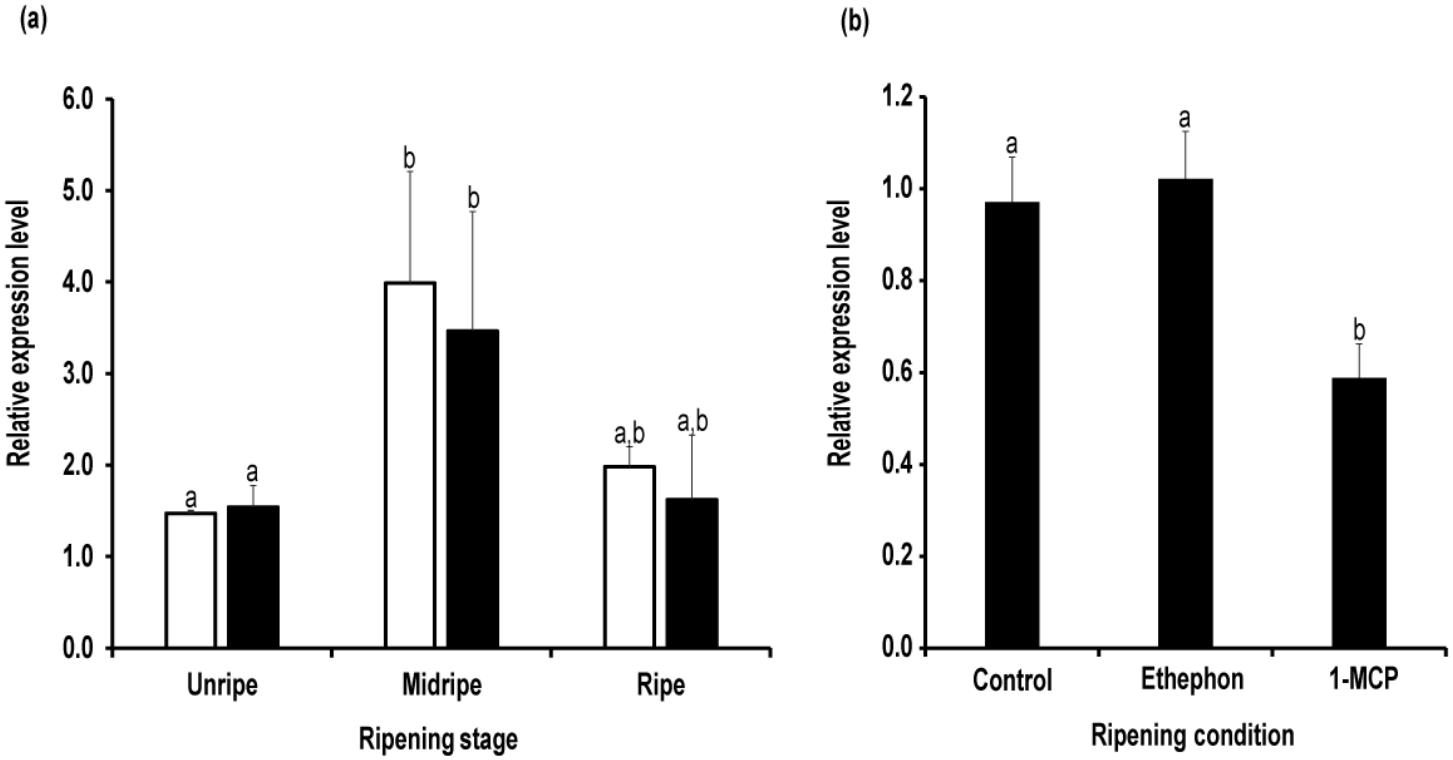

Figure 3

qRT-PCR analysis of DzLAP1 at various Chanee and Monthong cultivar ripening stages (a) and under different Monthong cultivar ripening conditions (b). DzLAP1 expression levels in durian pulp at unripe, midripe, and ripe stages in Chanee (white bars) and Monthong (black bars) cultivars (a) and under naturally ripening (control), ethephon treatment, and 1-MCP-treatment (b). Elongation factor 1 alpha (EF-1α) was reference gene. Bars: means ± standard deviation (SD) of three independent biological replicates. Different letters indicate significant differences based on Tukey's HSD multiple-range test ($p < 0.05$)

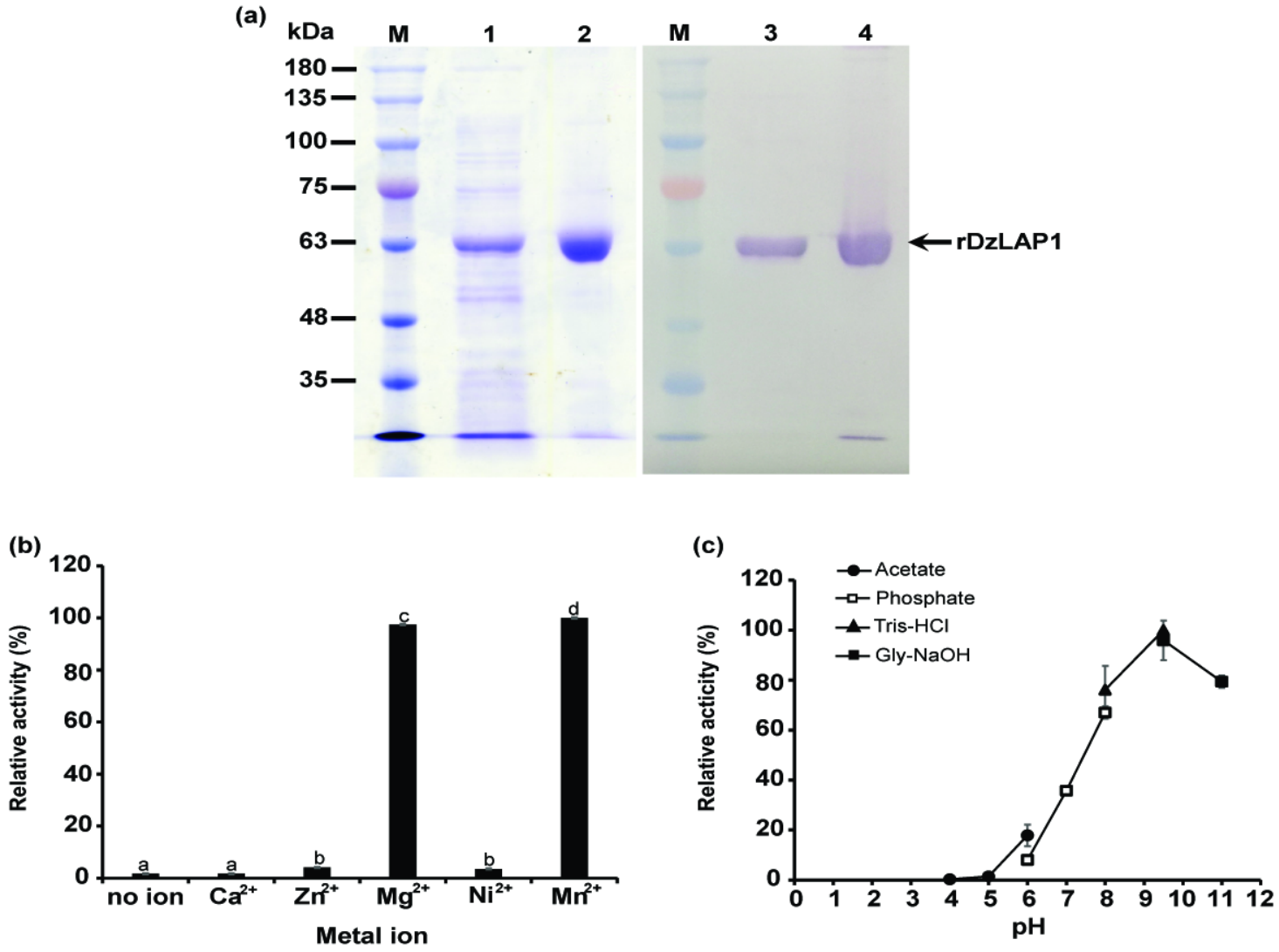

Figure 4

SDS-PAGE and western blot (a) metal ion dependency (b) and optimal pH (c) of recombinant DzLAP1. Lane M: standard protein ladder. Lanes 1 and 3: crude rDzLAP1. Lanes 2 and 4: purified rDzLAP1. Two micrograms each of crude and purified proteins were loaded onto SDS gel (a). Three and one-half micrograms rDzLAP1 was incubated with 7.5 mM Cys-Gly in 25 mM K3PO4 buffer (pH 7.2) in presence of 0 mM and 1 mM Ca2+, Zn2+, Mg2+, Ni2+, and Mn2+ at 37 °C for 15 min. Total reaction volume: 50 µL. Enzyme activity measured by modified acidic ninhydrin method [63] with spectrophotometric recording at 560 nm (A560) (b). Optimum pH of rDzLAP1 established by incubating 3.5 µg enzyme with 7.5 mM Cys-Gly and 1 mM Mg2+ at various pH (acetate buffer, pH 4 – 6; phosphate buffer, pH 6 – 8; Tris-HCl buffer, pH 8 – 9.5; Glycine-NaOH buffer, pH 9.5 – 11) at 37 °C for 15 min (c). Enzyme activity calculated where maximum activity was set as 100%

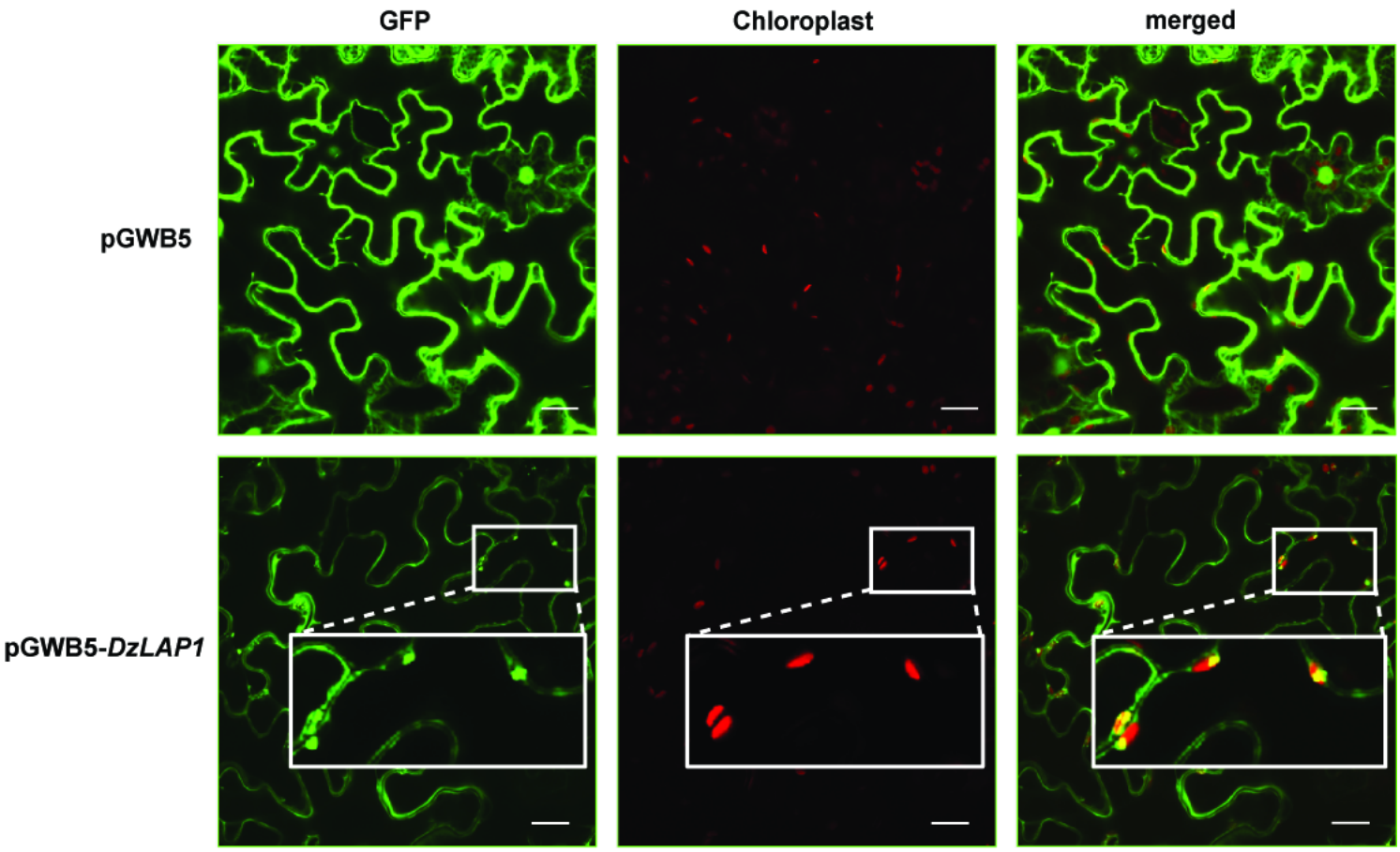

Figure 5

Subcellular localisation of GFP-tagged DzLAP1 in Nicotiana benthamiana leaves. Confocal microscopic images of N. benthamiana leaf epidermal cells infiltrated with pGWB5 (control; upper panel) and pGWB5-DzLAP1 (lower panel). GFP fluorescence (GFP), chloroplast autofluorescence (chloroplast), and merged images are shown. Plastidial DzLAP1-GFP localisation is shown at higher magnification in the insets. Scale bars: 20 µm

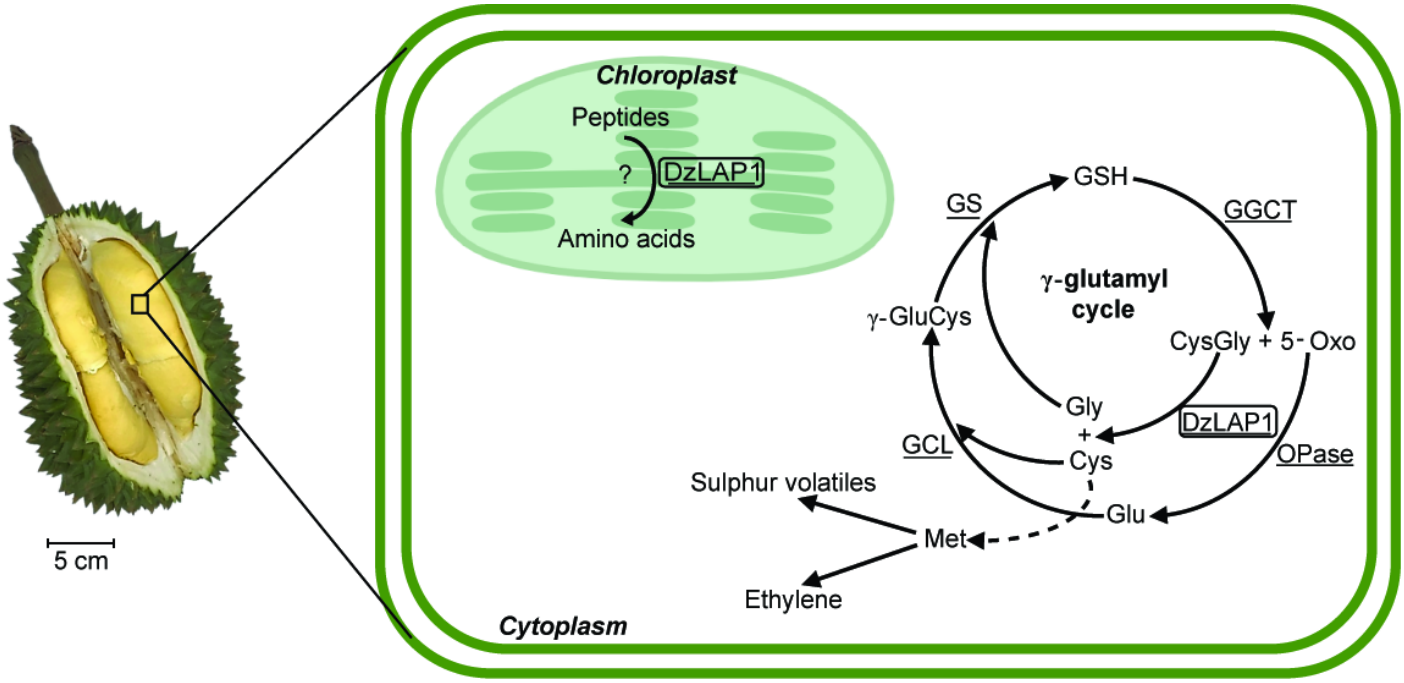

Figure 6

Schematic representation of putative DzLAP1 functions in two subcellular compartments of durian fruit pulp. DzLAP1 resides in both chloroplast and cytoplasm in the γ-glutamyl cycle (boxes). Broken lines indicate that > 1 reaction is involved. All enzymes are underlined. Abbreviations: DzLAP1: leucylaminopeptidase1; GGCT: γ-glutamylcyclotransferase; OPase: oxoprolinase; GCL: glutamate cysteine ligase; GS: GSH synthase; 5-Oxo: 5-oxoproline

Supplementary Files

This is a list of supplementary files associated with this preprint. Click to download.

- SupplementFigS2.tif
- SupplementaryTableS1.docx
- SupplementFigS1.tif